Appendix 1.1. Satellite photo showing study sites

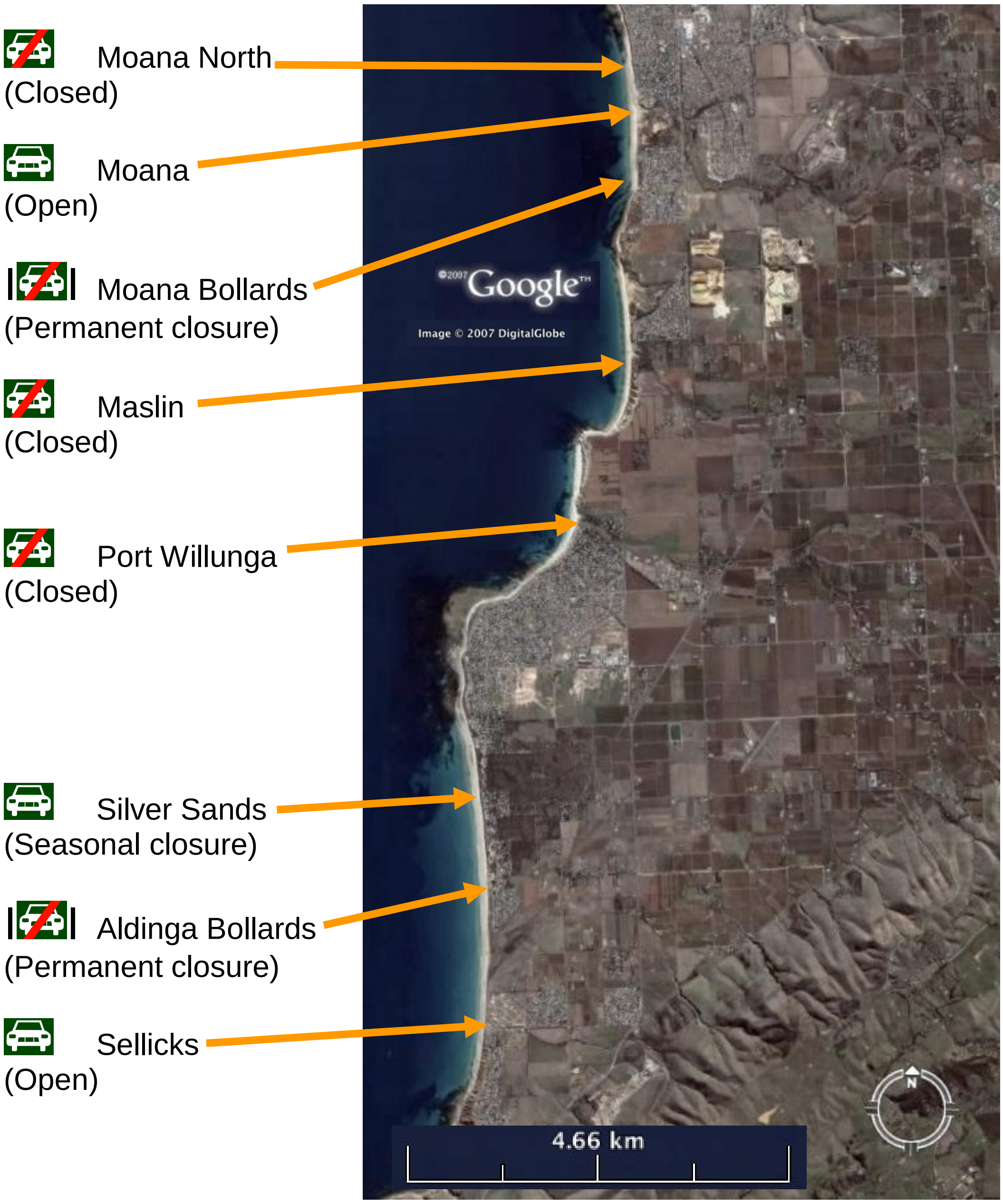

Note:

Moana North, Moana and Moana Bollards form one continuous stretch of beach in Moana Bay

Silver Sands, Aldinga Bollards and Sellicks form one continuous stretch of beach in Aldinga Bay

Normanville is located approximately 15km south of Sellicks beach

Appendix 1.2. Summary Table of site attributes for each beach or beach section sampled

	Moana North	Moana	Moana Bollards	Maslin	Port Willunga	Silver Sands	Aldinga Bollards	Sellicks	Normanville
General information									
Location	35.195S 138.469E	35.200S 138.470E	35.207S 138.470E	35.233S 138.470E	35.258S 138.461E	35.295S 138.445E	35.302S 138.446E	35.319S 138.447E	35.447S 138.306E
Length (km)	1.00	0.85	0.60	2.50	1.70	1.80	0.14	3.00	2.00
Grain size (μm)[1]	250.5	243.0	229.7	368.3	344.7	205.3	212.1	238.9	316.2
Slope (rise/run)[1]	0.041	0.051	0.040	0.063	0.044	0.041	0.045	0.062	0.062
Morphotype[2]	LTT/TBR	LTT/TBR	LTT/TBR	LTT/TBR	R+rocks+LTT	LTT	LTT	LTT	LTT
Notes on the Backshore and surrounds									
Backing	cliff/road	dunes	dunes	dunes/cliff	dunes/cliff	dunes/road	dunes	cobble bed	dunes
Surrounds	urban	wetland	urban	rural	semi-rural	urban	urban	semi-rural	semi-rural
Man-made defences	seawall	none	none	none	none	none	none	none	none
Creek	no	yes	no	yes	yes	no	no	yes	yes
Vehicle access									
Allowed	no	yes – all year	no – bollarded	no	no	seasonal – Oct. – May	no – bollarded	yes – all year	boat launch only
# car parks	1	1	1	2	1	1	0	2	1
# ramps	0	1	0	1 (locked)	1 (locked)	1	0	2	1

[1] average of all measurements taken over 3 years (see Chapter 3 for measurement details and methods)
[2] as stated in Short 2006a (R: reflective; LTT: low-tide terrace; TBR: transverse bar and rip)

Appendix 1.3. Photographs of study sites

Moana Bay Beaches: Looking south, Moana North in foreground, Moana and Moana Bollards in the background

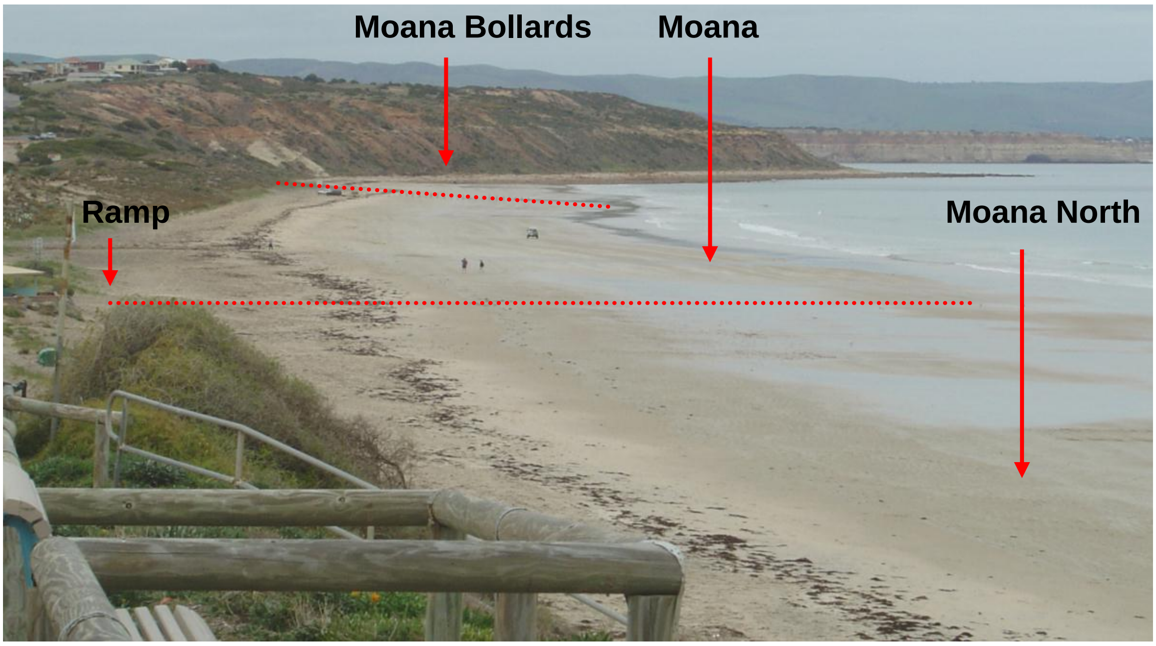

Maslin Beach, looking south, southern section

Port Willunga Beach (looking north, southern and northern sections visible)

Aldinga Bay Beaches: Looking south, Silver Sands (foreground), Aldinga Bollards and Sellicks in the background

Silver Sands/Aldinga Bollards/Sellicks, looking south

Normanville Beach, south of the jetty, looking south

Appendix 1.4: Daily wind speed ($km.h^{-1}$; blue series), rainfall (mm; red series) and maximum air temperature (°C; purple series) observations for Port Noarlunga, July 2005 – March 2008. Grey shading indicates periods for which there is no weather data available. Major sampling events (see Chapter 4, 5) are shown, also deployment period for markers (see Appendix 4.1). Storm events were classed as times when winds were greater than 80km/h (orange stars).

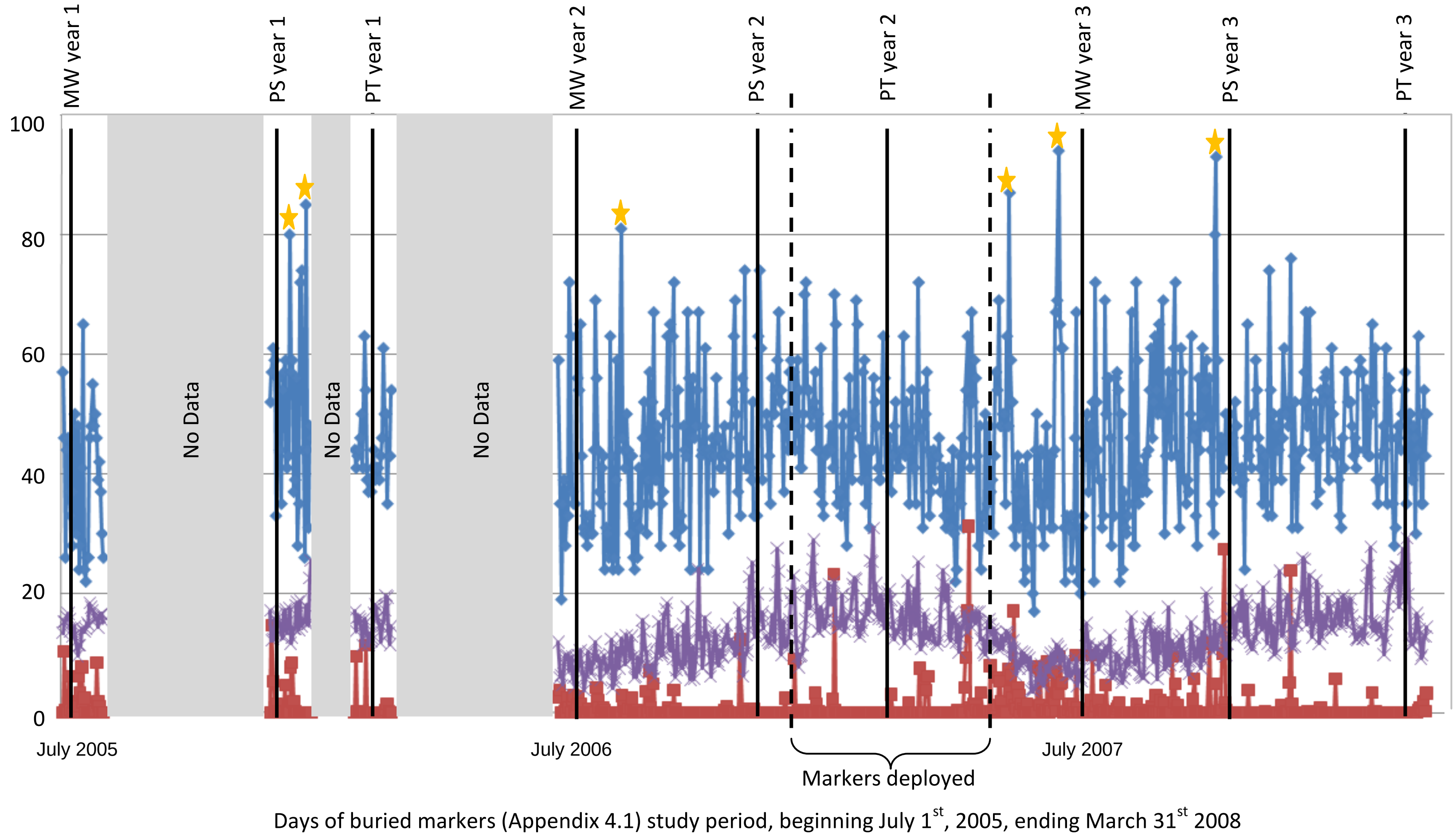

Appendix 3.1

Sieving versus laser-diffraction techniques for assessing grain-size distributions of beach sands

Tanith M. Ramsdale[†] and Peter G. Fairweather[†]

[†]Flinders University
School of Biological Sciences
GPO Box 2100 Adelaide, S.A., 5001, Australia
Tanith.Ramsdale@flinders.edu.au

LRH: Ramsdale & Fairweather
RRH: Comparing grain-sizing methods for beach sands

ABSTRACT

Laser diffraction analysis to determine grain-size distribution of sediments is a faster process than test-sieve methods; however, the results of these analysis methods can often differ. Samples are generally only analysed using one method, and so the need to convert results, such as for comparison to published values, may arise. This may also be the case when new analysis techniques become available to researchers during the course of a long term study. To determine a calibration equation for the comparison of results obtained by laser-diffraction to those from test sieves, natural beach-sand samples were processed by both methods, and the results for mean grain size, sorting, skewness and kurtosis were compared. There was a strong, linear relationship between the two methods for mean grain-size values. Laser-diffraction resulted in coarser mean grain-size values by 11.5-33.5% (mean = 25%). Samples processed by laser-diffraction had wider grain-size distributions (indicating poorer sorting), but there was also a strong, linear relationship between sorting values obtained by both methods. Grain size distributions were more symmetrical and more peaked compared for laser diffraction compared to test sieve-derived values. For the beach sand samples processed, laser-diffraction offers a faster method for calculation of mean grain size, with the tight mathematical relationship between mean grain size and sorting values obtained by the two methods tested allowing comparison of laser-diffraction values to test-sieve derived values, if needed. Values for sorting, skew and kurtosis may be affected by smoothing calculations within the laser-diffraction particle sizing software.

ADDITIONAL INDEX WORDS: *calibration equation, dry sieving, graphical comparison, laser granulometry, South Australian beaches, test sieve*

INTRODUCTION

Sieve analysis of dried samples has been the standard method for determining the grain-size distribution of coarser sediments, such as beach sands, where the amounts of fine sediments (i.e. clays and silts) are negligible. Usually, 25 - 100g of pre-dried sediment is placed in a stack of Wentworth grade test-sieves and mechanically shaken for a fixed-time period (BALE and KENNY 2005). Processing samples in this way is a long and laborious task. Where a large number samples are collected, as is the case for large-scale ecological investigations, many weeks may be required to process all the samples for grain-size distribution.

Laser diffraction is another method by which sediment samples may be processed for grain-size distribution (BLOTT and PYE 2006). A smaller sample is required, generally only 5 - 10g, which is diluted in water and passed through a measurement cell. A focused laser beam then passes through the sample and the resulting forward-scattering pattern of the laser by the suspended particles is measured by a detector array. Mie and/or Fraunhofer theories are then used to process the scattering pattern angle and intensity data into a grain-size distribution (BALE and KENNY 2005). This method has the advantage of rapidly and precisely measuring the size-distribution of particles in a sample over a large range (MCCAVE and SYVITSKI 1991; BLOTT and PYE 2006). The use of standard operating procedures reduces operator error, increases accuracy and makes it possible to compare results obtained on different instruments (BALE and KENNY 2005). The use of laser-diffraction in ecological investigations is becoming increasingly common (e.g. CIUTAT *et al.* 2006; DITTMANN *et al.* 2006a;b; MASSELINK *et al.* 2007); however, the expense of purchasing and then maintaining the instrumentation is restrictive.

Results obtained by laser-diffraction techniques differ from those obtained through more traditional techniques. Underestimation of the clay content and overestimation of the silt content of fine-grained sediments compared to pipette methods has been observed (MCCAVE *et al.* 1986; SINGER *et al.* 1988; KONERT and VANDENBERGHE 1997; RAMASWAMY and RAO 2001). This problem is overcome by adjusting the grain-size level for the clay-silt boundary (KONERT and VANDENBERGHE 1991; RAMASWAMY and RAO

2001). Sand samples analysed by laser-diffraction have been classed as coarser than when processed by sieve methods (KONERT and VANDENBERGHE 1997; BLOTT and PYE 2006; RODRIGUES & URIARTE 2009), with increasing differences in results obtained by the two methods partially attributed to increasing degrees of particle non-sphericity (BLOTT and PYE 2006). Also, because laser-diffraction software algorithms include smoothing procedures to obtain log-normal grain-size distributions, other distributions (i.e. asymmetric or bimodal) may be misrepresented, and calculations of skew and kurtosis may be of little use, regardless of particle shape (BLOTT and PYE 2006).

Open-ocean beach sands provide a good model for the comparison of different methods for determining grain-size distribution statistics. Beach sands tend to be well-sorted by the surf, with sediment sources, wave types and off-shore slope determining which grain sizes are predominantly deposited onto a particular beach (KOMAR 1976). Beach sands also contain minimal amounts of clay and silt (KOMAR 1976), which, aside from being misrepresented in laser-diffraction analysis, can also cause problems due to flocculation (KONERT and VANDENBERGHE 1997). Micas (sand-sized flat particles that have been shown to significantly reduce the estimated grain-size of sand samples; HAYTON *et al.* 2001) are also uncommon in beach sands because wave energy holds these particles up in suspension, preventing their deposition on the intertidal beach (KOMAR 1976).

When new analysis techniques are introduced during long-term studies, it is essential that the results from the old and new method are comparable (SHILLABEER *et al.* 1992). In order to compare results obtained by laser-diffraction and test-sieve particle sizing methods, calibration factors need to be developed. For instance, a method for the inter-conversion of light diffraction (using a Microtrac instrument) to equivalent test-sieve size distributions using quartz and finely-ground coal samples has been developed (AUSTIN and SHAW 1992). SHILLABEER *et al.* (1992) used natural sediments, inter- and sub-tidal in origin, to develop a mathematical model for the comparison of laser-diffraction versus test-sieve derived values for particle sizing. These authors noted that it was not appropriate to apply a single conversion factor for all sediment samples due to differences in sediment types and size classes, and so presented conversion factors for samples based on eight sediment distributional types (SHILLABEER *et al.* 1992).

Sediment studies on intertidal sandy beaches need to give an accurate and comparable representation of grain size distribution; sediment grain size is an important indicator of beach morphotype (SHORT 2006a) and predicts the abundance and diversity of macroinvertebrate communities (MCLACHLAN and DORVLO 2005). Changes in sediment-processing methods that result in apparent differences in grain-size distributions due only to the analysis technique used could, thus, be falsely interpreted as shifts in beach morphology or ecology. Alternatively, differences in results obtained by two methods could obscure particle-size distribution shifts (SHILLABEER *et al*. 1992). Previously-developed conversion factors for laser-diffraction and test-sieve data (SHILLABEER *et al*. 1992) did not include one that represents the sediment distribution type observed in the fine-medium sands on the microtidal high-energy sandy beaches along the Fleurieu Peninsula and southern metropolitan coastline of South Australia (Table 1). Therefore, the aim of this paper is to create a calibration equation for use with intertidal sediments collected from these beaches, which allows comparison of laser diffraction-derived data to results obtained by using traditional test-sieve analysis.

METHODS

Samples

Sediment core samples were collected from six open-ocean microtidal beaches along the Fleurieu Peninsula and metropolitan Adelaide coastlines, south of Adelaide, South Australia, representing a range of typically medium through to fine sand beaches (SHORT 2006b; Table 2). Most beaches were sampled as part of an ongoing investigation by the authors assessing the ecological impacts of vehicles on sandy beaches in southern metropolitan Adelaide, with the addition of two sites from the Fleurieu Peninsula in an attempt to encapsulate the full range of grain-sizes of the beaches in this region. Samples were collected using a 10.5cm-diameter PVC corer to 10cm depth, and stored at 0°C for immediate processing. For each sample, approximately 100g of the homogenised sediment was dried to constant weight at 80°C for 24 hours. No pre-treatment of the samples, to remove carbonates or organic matter, was performed, because the beaches in this region generally contain carbonate sands (average of 67±32% carbonate content; SHORT 2006a), and so removal of carbonates may have significantly altered the grain-size distribution of the samples. Organic matter content of the samples, determined from a separate sub-sample of the original homogenised sediment core was very low (range 0.117–3.194% DW; mean = 0.846%) and so sediment pre-ashing to remove organic matter was not performed.

Test-sieve Method

Each dried 100g sediment sample was placed in a nest of six Wentworth graded test-sieves (2mm, 1mm, 500μm, 250μm, 125μm, 63μm plus collection pan <63μm) and shaken in a mechanical shaker for 15 minutes, after which the sediment retained on each sieve and in the collection pan was weighed (BALE and KENNY 2005). The percentage of the sample retained in the collection pan ranged between 0.001-0.116%, with an average of only 0.039%, and thus a separate analysis of the silt-clay fraction was not performed. The fractions were recombined and each sub-sample stored in an air-tight, zip-locked plastic bag.

Laser Diffraction Method

The recombined sub-samples from the test-sieve analysis were used for laser diffraction, thus allowing direct comparison of the grain-size data between the two methods. Because samples processed for laser-diffraction in this study were irretrievable, laser-diffraction was always conducted after test-sieving. A Malvern Mastersizer instrument, with a Hydro2000 attachment dispersal unit (using deionised water as the dispersal medium), was used to perform laser-diffraction analysis. Although the Mastersizer instrument is capable of detecting and measuring particles between 0.02μm and 2000μm, particles with a diameter greater than 1mm must be removed prior to processing to avoid damage to the pump of the dispersal unit. Thus, the recombined sample was sieved through a 1mm sieve. Calculation of the percentages of the sample processed by the Mastersizer and the fraction retained on the 1mm sieve enabled the data to be recombined for the calculation of grain-size distribution statistics. Approximately 5-10g of the remaining dry, homogenised sediment was placed directly into deionised water in the dispersal unit at a set pump speed of 3500rpm and target obscuration of the laser beam of 7-10%. Finer sands tended to require less sediment by weight to reach the target obscuration, but there was no relationship between mean grain size and the weight of sample required ($R^2 = 0.03$; $p = 0.22$). Flocculation problems were not experienced due to the small amounts of clays and silts. Initially three sub-samples were analysed per sample, but this was deemed unnecessary and was therefore reduced to one, because the results for each sub-sample were similar (within 0.18–3.54%). The standard operating procedure specified by the manufacturer of the Mastersizer (i.e. 5 measurements, each approximately 2000 snapshots of the sediment light scattering pattern, with no pause between measurements; MALVERN INSTRUMENTS 2007) was found to be appropriate for the beach sands analysed in this study. The average of the five measurements was used to calculate grain-size distribution statistics.

Statistics

Fraction weights obtained from test-sieve analysis were analysed using the GRADISTAT software (BLOTT and PYE 2001) to obtain geometric mean grain-size, sorting, skewness and kurtosis (method of moments). For laser-diffraction data, percent finer data (i.e. the total percentage of the sediment grain-size distribution that is finer than a particular interval) in quarter-phi intervals (i.e. 21 logarithmic intervals from 63 – 2000μm) were extracted from the Malvern software and these values were used to calculate the percentages contained within each quarter-phi size bracket. The percentage of the sample retained on the 1mm sieve before laser-diffraction analysis was calculated and the quarter-phi percentages were calibrated to represent the remainder of the sample (i.e. the percentage < 1mm). These data were then processed through the GRADISTAT software (BLOTT and PYE 2001) to allow comparisons to test-sieve derived values. Scatterplots of laser-diffraction values versus test-sieve values for each comparison were constructed and regression analysis was used to test the strength of any linear relationships observed, using laser-diffraction values as the dependent variable and test-sieve values as the independent variable.

RESULTS

Processing samples by laser-diffraction was more rapid than sieving. With two complete sets of test sieves in use, so that one set could be shaken while the second was emptied and the fractions weighed, three sediment samples could be processed in approximately one hour. Twice as many samples could be processed by laser-diffraction in approximately 45 minutes, under half the time required to sieve per sample. Also, results obtained by laser-diffraction were automatically recorded and stored by the Malvern software; thus no additional time was required for data entry and checking.

In total, 45 samples were processed by each method. Of the grain-size frequency-distribution plots obtained by test-sieve methods, 62% were classed as bimodal distributions by GRADISTAT, and a further 11% classed as trimodal. Only one of the 45 distribution plots of laser-diffraction data was bi-modal. The average grain-size percent composition indicated that the samples contained predominantly fine sands, with only small amounts of finer particles (Table 1).

Mean Grain size

Laser-diffraction values for mean grain size were greater (i.e. coarser) and spread over a wider range (i.e. 155 - 412μm) than values obtained by test-sieve analysis (range 126 - 287μm) on the same samples (Table 3). Laser-diffraction results indicated a coarsening of grain-size measurements by 11.5 to 33.5% (mean = 25.0%). A scatterplot of laser-diffraction versus test-sieve-derived values indicated a strong linear relationship (Figure 1). Boxplots of each variable indicated slightly positively skewed data (Figure 1); however, the residuals of the linear regression analysis were evenly spread and removal of one outlier identified during the analysis did not affect the result. The relationship between the two sets of values was strong and highly significant (Table 3), indicating that there was a high degree of linear predictability between the two variables. The results lie above the 1:1 line (Figure 1), with points moving further from this line with increased estimated mean grain-size, indicating that laser-diffraction analysis overestimate mean grain-size, and that the degree of overestimation increases with increasing grain size. The classical Udden/Wentworth (UDDEN 1914; WENTWORTH 1922) sediment grade scale was then calibrated for laser-diffraction data using the regression equation, resulting in coarsening of the transition points between the different sand classes and the silt/clay – sand boundary (Table 4).

Grain-size distribution statistics

Boxplots for each variable (i.e. sorting, skewness and kurtosis) indicated that most data sets were slightly skewed, but again in all regression analyses the residuals were evenly spread and removal of identified outliers did not alter the results (Figure 2). Values for sorting obtained from test-sieve data were small, between 1.17 and 1.73 (Figure 2a), classing samples as very well to moderately well-sorted (BLOTT and PYE 2001). Laser-diffraction values for the same samples were similar (1.29 – 1.64; well sorted – moderately well sorted). A scatterplot of values obtained by the two methods indicated a strong linear relationship, which was found to be significant by linear regression analysis (Figure 2a, Table 3). In order to determine if there was any difference in the degree of sorting for each individual sample, percentile values (D_{10} and D_{90}) calculated by GRADISTAT were used to compare the sample distribution widths (i.e. wider distribution indicates poorer sample sorting; BLOTT & PYE 2006). With the exception of one case (a sample with 4.7% of grains >1mm), the grain-size distributions were wider for laser-diffraction-derived data (i.e. above the 1:1 line; Figure 2b), indicating measurement of poorer sorting for samples when processed by laser diffraction.

Skewness values close to zero indicate more symmetrical distributions, with negative and positive values representing fine- and coarse-skewed data, respectively (BLOTT and PYE 2001). Values obtained from laser-diffraction analysis indicated improved symmetry in comparison to test sieve-derived values (Table 3). There was a significant linear relationship between the values obtained by both methods (Table 3), but the slope for the relationship was less than one, indicating a lack of covariance, which was also observed in the scatterplot (Figure 2c).

Increasing values for kurtosis indicate more peaked distributions (Blott and Pye 2001). Grain-size distributions from laser-diffraction analysis were more peaked (Table 3). There was no linear relationship between test-sieve and laser-diffraction values for kurtosis (Figure 2d), with laser diffraction returning too small a range of values in comparison to test-sieve analysis of the same samples.

DISCUSSION

Values for mean grain size obtained from laser-diffraction correlated strongly with test-sieve values. Laser-diffraction values for calibrated cut-off points of grain-size classes were greater than those for test-sieve analysis results (Table 4). This result is an indication of particle non-sphericity of the beach sands used (Konert and Vandenberghe 1997). Laser diffraction derived grain size distribution statistics indicated increased sample distribution widths (poorer sorting) but improved symmetry and peakedness compared to test-sieve derived values. Sorting values obtained by the two methods were also strongly correlated but skewness and kurtosis were very poorly correlated and unrelated, respectively. Rodriguez and Uriarte (2009) undertook a similar study using subtidal marine sediments. These authors compared grain size distribution statistics obtained by test sieving to those obtained by laser diffraction using a Beckman-Coulter LS 13 320 instrument which uses the Fraunhofer diffraction model . These authors found that, for a different instrument that uses a different theory, there was also a very poor correlation between test-sieve and laser diffraction derived values for skew and kurtosis, but that mean-grain size and sorting values were strongly correlated (Rodriguez and Uriarte 2009).

Calibrated grain-size classes show that laser-diffraction overestimated the size of the sand grains, with laser-diffraction values for mean grain size of the samples being between 11.5% and 33.5% coarser than test-sieve-derived values. Particle shape, specifically particle non-sphericity, has been shown previously to significantly affect the determination of grain-size for sand-sized particles (KONERT and VANDENBERGHE 1997; BLOTT and PYE 2006). Laser analysis (using a Fritsch A22 instrument) of aeolian-derived sand particles (diameters >63μm) gave coarser results by 9-20% than values obtained by test-sieve methods (KONERT and VANDENBERGHE 1997). Non-sphericity of the natural sand grains was hypothesised to be reason for the observed difference – the equivalent volume diameter of an irregular particle (i.e. the property measured by laser diffraction) is greater than the width or *b*-axis (i.e. the property measured by test-sieve mesh), resulting in deviation between the results of the two methods, depending on the degree of non-sphericity (KONERT and VANDENBERGHE 1997). Natural sand samples processed by laser analysis, using a Beckman-Coulter LS230 Rapid VUE instrument, were found to be between 8-26% coarser than results obtained by dry sieving, with particle sphericity partially responsible for the observed differences (BLOTT and PYE 2006). Increased particle sphericity resulted in decreased differences in results obtained for laser-diffraction and dry sieving, again indicating that laser-diffraction overestimates the size of irregular particles (BLOTT and PYE 2006). It is likely that the non-sphericity of the natural beach sands used in this study have caused the observed off-set of results for mean grain size measured by the two methods.

In terms of rapidity and repeatability, laser-diffraction is superior for the calculation of mean grain-size. Most distribution statistics improved when analysed by laser diffraction. Test-sieve data plots indicated moderately- to well-sorted samples, although 73% were classed as either bi- or tri-modal, ranging from very fine to very coarse skewed and flat to reasonably peaked in shape. Laser-diffraction data indicated the same samples had less well-sorted and wider grain-size distributions, but the distributions were almost entirely unimodal in nature, more symmetrical and more peaked. However, it is important to note that this apparent improvement is at least partly due to the algorithms used by laser-diffraction software that smooth the data into a log-normal distribution, resulting in altered skew, suppressed kurtosis and degraded sorting values (BLOTT and PYE 2006). Well-sorted beach sands should have a high degree of log-normality in their grain-size distributions, with single peaks and narrow ranges; however, the large differences between beach-sand samples processed by the two methods in this study indicate that if sorting, skew and kurtosis estimates are required, then test-sieve analysis should be conducted.

Although the mean-grain size of the sand samples measured by laser-diffraction was greater than in the test-sieve analysis, the strong mathematical relationship between results obtained by the two different methods makes calibration of results from laser-diffraction to test-sieve values straightforward. Using the calibration equation also makes it possible to compare sand mean grain sizes from different studies that utilised test-sieve methods with values obtained in this study by laser diffraction. The calibration equation developed for beach sands in this study should be applicable where sands are similar in grain-size distribution type (i.e. Table 1), with almost no clay/silt (e.g. less than 1%) and only a small percentage (less than 5%) of grains greater than 1mm in size.

ACKNOWLEDGEMENTS

T.M.R. would like to thank all field assistants involved in this study. This research was supported by funding from the Onkaparinga City Council and the Flinders Research Centre for Coastal and Catchment Environments. Thank-you also to R. Lester, R. Langley, S. Duong and J. Blatchford for their helpful comments, which greatly improved the draft version of this manuscript.

LITERATURE CITED

AUSTIN, L.G. & SHAW, I., 1992. A method for inter-conversion of Microtrac and sieve size distributions. *Powder Technology*, 35, 271-278.

BALE, J.J. & KENNY, A.J., 2005. Sediment analysis and seabed characterisation. *In:* A. ELEFTHERIOU and A. MCINTYRE (eds.), *Methods for the study of the marine benthos.* New Delhi, India: Blackwell Science Ltd., pp. 43-86.

BLOTT, S.J. & PYE, K., 2001. GRADISTAT: A grain size distribution and statistics package for the analysis of unconsolidated sediments. *Earth Surface Processes and Landforms*, 26, 1237-1248.

BLOTT, S. J. & PYE, K., 2006. Particle size distribution analysis of sand-sized particles by laser diffraction: an experimental investigation of instrument sensitivity and the effects of particle shape. *Sedimentology*, 53, 671-685.

CIUTAT, A., WEBER, O., GERINO, M. & BOUDOU, A., 2006. Stratigraphic effects of tubificids in freshwater sediments: a kinetic study based on X-ray images and grain-size analysis. *Acta Oecologica-International Journal of Ecology*, 30, 228-237.

DITTMANN, S., CANTIN, A., IMGRABEN, S. & RAMSDALE, T., 2006a. *Macrobenthic Survey 2005: Murray Mouth, Coorong and Lower Lakes RAMSAR site*. Adelaide, South Australia: Report for the Department of Environment and Heritage. 33p.

DITTMANN, S., CANTIN, A., IMGRABEN, S., RAMSDALE, T. & POPE, A., 2006b. *Effects of water release across the Ewe Island and Boundary Creek barrages, September 2005, on benthic communities in mudflats of the River Murray estuary*. Adelaide, South Australia: Report for the Department of Environment and Heritage. 26p.

FOLK, R. L. & WARD, W. C., 1957. Brazos river bar: a study in the significance of grain size parameters. *Journal of Sedimentary Petrology*, 27, 3-26.

HAYTON, S., NELSON, C. S., RICKETTS, B. D., COOKE, S. & WEDD, M. W., 2001. Effect of mica on particle-size analyses using the laser-diffraction technique. *Journal of Sedimentary Research*, 71, 507-509.

KOMAR, P. D., 1976. *Beach processes and sedimentation*. New Jersey: Prentice-Hall Inc. 429p.

KONERT, M. & VANDENBERGHE, J., 1997. Comparison of laser grain size analysis with pipette and sieve analysis: A solution for the underestimation of the clay fraction. *Sedimentology*, 44, 523-535.

MALVERN INSTRUMENTS, 2007. *Mastersizer 2000 user manual*. England: Malvern Instruments Ltd.

MASSELINK, G., AUGER, N., RUSSELL, P. & O'HARE, T., 2007. Short-term morphological change and sediment dynamics in the intertidal zone of a macrotidal beach. *Sedimentology*, 54, 39-53.

MCCAVE, I.N. & SYVITSKI, J.P.M., 1991. Principles and methods of geological particle size analysis. *In:* J.P.M. SYVITSKI (ed.), *Principles, methods* *and application of particle size analysis.* Cambridge: Cambridge University Press, pp. 4-42.

McCave, I. N., Bryant, R. J., Cook, H. F. & Couchanowr, C. A., 1986. Evaluation of a laser-diffraction-size analyser for use with natural sediments. *Journal of Sedimentary Petrology*, 56, 561-564.

McLachlan, A. & Dorvlo, A., 2005. Global patterns in sandy beach macrobenthic communities. *Journal of Coastal Research*, 21, 674-687.

Quinn, G.P. & Keough, M.J., 2002. *Experimental design and data analysis for biologists.* Cambridge: Cambridge University Press, 537p.

Ramaswamy, V. & Rao, P. S., 2006. Grain size analysis of sediments from the northern Andaman Sea: Comparison of laser-diffraction and sieve-pipette techniques. *Journal of Coastal Research*, 22, 1000-1009.

Rodriguez, J.G. & Uriarte, A. 2009. Laser diffraction and dry-sieving grain size analysis undertaken on fine- and medium-grained sandy marine sediments: A note. *Journal of Coastal Research*, 25, 257-264.

Shillabeer, N., Hart, B. & Riddle, M., 1992. The use of a mathematical model to compare particle size data derived by dry-sieving and laser analysis. *Estuarine, Coastal and Shelf Science*, 35, 105-111.

Short, A.D., 2006a. Australian beach systems - Nature and distribution. *Journal of Coastal Research*, 22, 11-27.

Short, A.D., 2006b. *Beaches of the South Australian coast and Kangaroo Island: A guide to their nature, characteristics, surf and safety.* Sydney, New South Wales: Sydney University Press, 346p.

Singer, J. K., Anderson, J. B., Ledbetter, M. T., McCave, I. N., Jones, K. P. N. & Wright, R., 1988. An assessment of analytical techniques for the size analysis of fine-grained sediments. *Journal of Sedimentary Petrology*, 58, 534-543.

Udden, J. A., 1914. mechanical composition of clastic sediments. *Bulletin of the Geological Society of America*, 25, 655-744.

Wentworth, C. K., 1922,). A scale of grade and class terms for clastic sediments. *Journal of Geology*, 30, 377 - 392.

Table 1 Average % composition of sediment grain-sizes for the beach sand samples used in this study

Sediment type	Size range (μm)	Average % Composition
Granules	≥ 2000	0.20
Very Coarse Sand	1000 – 1999	0.35
Coarse Sand	500 – 999	2.74
Medium Sand	250 – 499	27.18
Fine Sand	125 – 249	61.52
Very Fine Sand	63 – 124	7.95
Silt/Clay	≤ 62	0.04

Table 2. Beaches sampled for grain-size distribution comparisons in two regions, with their morphotype (as classified by SHORT 2006b: LTT, low tide terrace; TBR, transverse bar and rip; RBB, rhythmic bar and beach; D, dissipative), the number of samples from each beach (*N*), typical sand grain-size classification and mean organic matter content (OM%: as determined by loss on ignition analysis) of the samples processed. The number given in brackets next to the beach name is the reference number given by SHORT 2006b.

Beach	Region	Morphotype	*N*	Typical sand	Mean OM%
Aldinga (216)	Metro	LTT	30	Fine	0.683
Port Willunga (217)	Metro	LTT/TBR	3	Fine	0.565
Normanville (207)	Metro	LTT	3	Fine-medium	0.358
Maslin (219)	Metro	LTT/TBR	3	Fine-medium	0.699
Goolwa (149A)	Fleurieu	D	3	Fine	1.586
Waitpinga (170)	Fleurieu	RBB	3	Medium	2.649

Table 3. Regression relationship strength (values in bold indicate significance $p = 0.000$; otherwise NS $p > 0.05$), intercept and slope values for each comparison of laser-diffraction and test-sieve derived values for distribution statistics. Values for laser and sieve data both with and without the 1mm fraction reincorporated are given.

Statistic [1]	**Laser values range**	**Sieve values range**	R^2	**Intercept**	**Slope**
Mean (x_g)	155 - 412µm	126 - 287µm	**0.97**	-16.524	1.441
Sorting (σ_g)	1.29 - 1.64	1.17 - 1.73	**0.86**	0.496	0.654
Skewness (Sk_g)	-0.11 - 0.59	-3.16 - 2.34	**0.25**	0.068	0.065
Kurtosis (K_g)	2.45 - 5.48	2.79 - 23.36	0.001	*no sig. relationship*	

[1] Values for geometric method of moments grain size distribution statistics were obtained from fraction weights (sieve data) or percents (laser diffraction data) using the GRADISTAT software (BLOTT & PYE 2001).

Table 4. Calibrated laser-diffraction (CLD) values for the Udden/Wentworth grade-scale (UDDEN 1914; WENTWORTH 1922), determined for beach sands with minimal silt/clay in the study region. Although the Mastersizer 2000 is capable of measuring particles along the entire range of sand grades, the scale presented here has been calibrated using interpolation of the regression model, with mean values from test-sieve analysis between 126 - 287μm (i.e. Figure 1). Values outside this range have been extrapolated.

Broad description	Description and size (μm)		CLD size
Sand	*Very coarse sand*	2000	2865.5
	Coarse sand	1000	1424.5
	Medium sand	500	704.0
	Fine sand	250	343.7
	Very fine sand	125	163.6
Silt and clay fraction		< 62	< 72.8

Figure captions:

Figure 1. Scatterplot of mean grain-size estimated by laser-diffraction and test-sieve methods on the same samples (*N* = 45). The fitted line equals the regression given as the equation. The dotted line indicates the 1:1 line. Marginal boxplots show the sample distribution of each variable. The line inside the box is the median value, with the edges of the boxes indicating the range of points in the total distribution 25% above and below the median. The lines extend to extreme values (up to 1.5 the total width of the box) and crosses and circles indicate outliers (QUINN & KEOUGH 2002). Mean grain size values were estimated geometrically using FOLK & WARD (1957) method of moments in the GRADISTAT software (BLOTT & PYE 2001).

Figure 2. Scatterplots of sample: a) sorting; b) distribution width; c) skew; and d) kurtosis values estimated by laser-diffraction and test-sieve methods on the same samples (*N* = 45) (dotted line indicates 1:1 line). Regression equations relate test-sieve (TSV) and laser-diffraction values (LDV). Marginal boxplots, showing aspects of the sample distribution for each variable, are included. Sorting, skew and kurtosis values were estimated geometrically using FOLK & WARD (1957) method of moments in the GRADISTAT software (BLOTT & PYE 2001).

Figure 1.

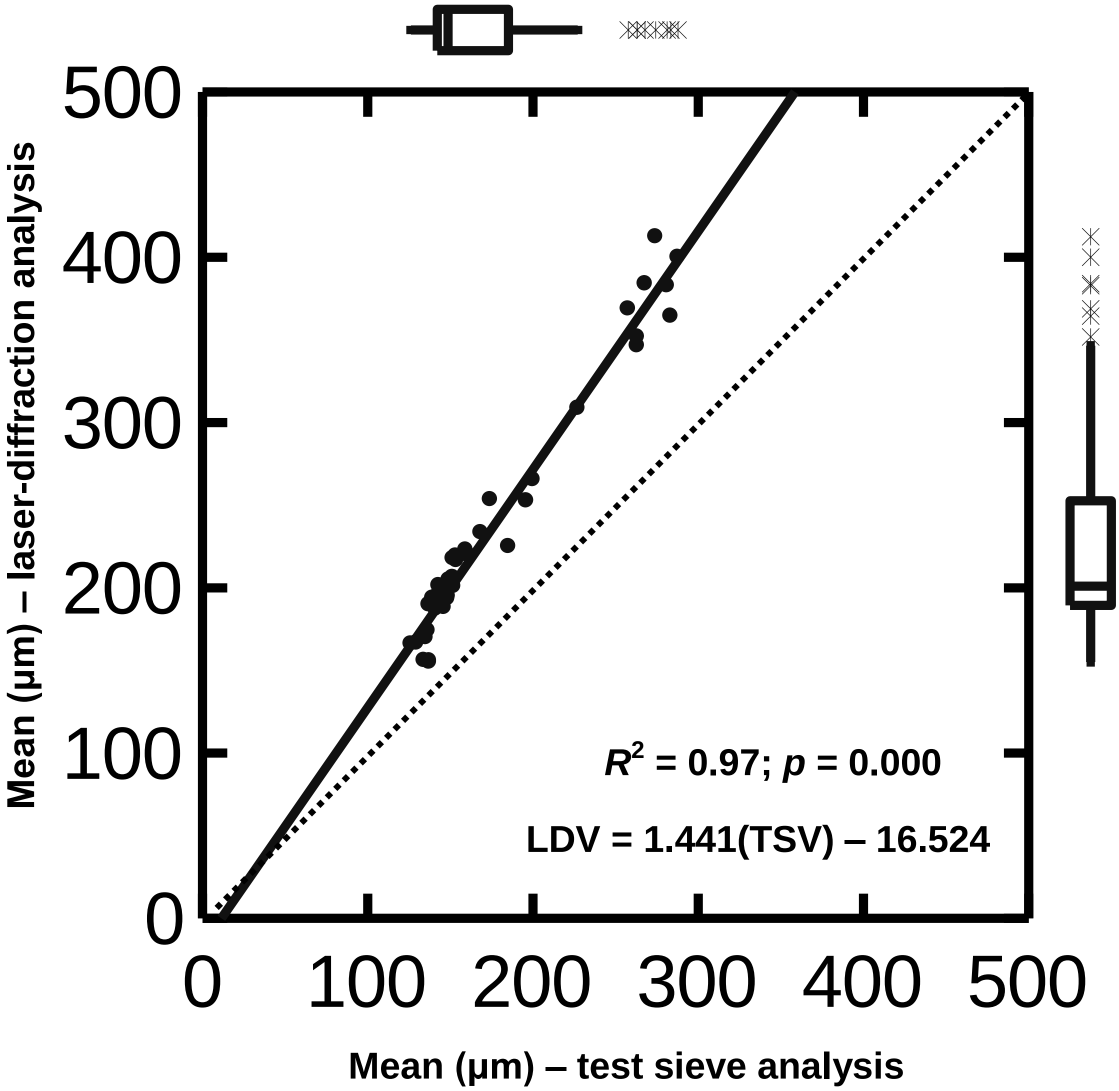

500
400
300
200
100
0
0
100
200
300
400
500
Mean (µm) – laser-diffraction analysis
Mean (µm) – test sieve analysis
R2 = 0.97; p = 0.000
LDV = 1.441(TSV) – 16.524

Figure 2.

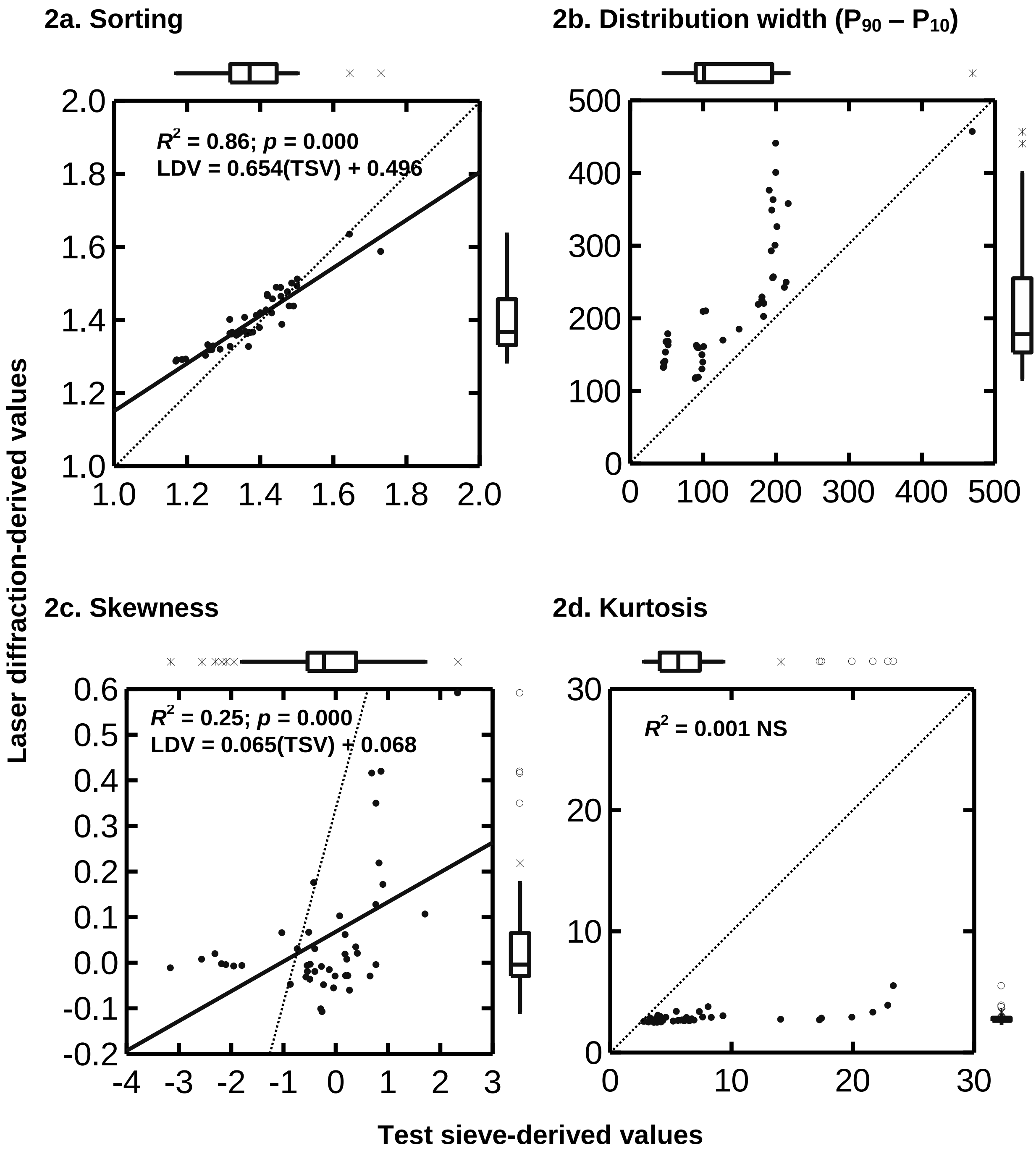
2a. Sorting
R^2 = 0.86; p = 0.000
LDV = 0.654(TSV) + 0.496
2b. Distribution width (P_{90} – P_{10})
2c. Skewness
R^2 = 0.25; p = 0.000
LDV = 0.065(TSV) + 0.068
2d. Kurtosis
R^2 = 0.001 NS
Laser diffraction-derived values
Test sieve-derived values

Appendix 3.2: Frequencies of cores with cobbles versus cores without cobbles between beaches open v closed to vehicles and results of contingency table tests for each sampling occasion (*n* = 9), year (*n* = 3) or season (*n* = 3). Bold text indicates significant associations between beach types and cobble presence or absence. In this case, there is frequently an association between open beaches and cobble presence in sediment cores. There was no data (n/d) for the pre-summer sampling occasion in year 3 because sediment cores were not collected on that occasion.

a) 2x2 tables		Year 1		Year 2		Year 3		Overall	
		Absent	Present	Absent	Present	Absent	Present	Absent	Present
Mid-winter	Closed	25	11	**35**	**1**	**33**	**3**	**93**	**15**
	Open	18	18	**22**	**14**	**24**	**12**	**64**	**44**
Pre-summer	Closed	28	8	31	5	n/d		**59**	**13**
	Open	40	16	26	10			**46**	**26**
Post-summer	Closed	32	4	29	7	33	3	94	14
	Open	29	7	27	9	27	9	83	25
Overall	Closed	**85**	**23**	**95**	**13**	**66**	**6**	**246**	**42**
	Open	**67**	**41**	**75**	**33**	**51**	**21**	**193**	**95**

b) Fishers Exact test statistics	Year 1	Year 2	Year 3	Overall
Mid-winter	0.149	**<0.001**	**0.018**	**<0.001**
Pre-summer	0.628	0.245	n/d	**0.024**
Post-summer	0.514	0.778	0.111	0.076
Overall	**0.011**	**0.001**	**0.002**	**<0.001**

Appendix 3.3: Frequency of cores with cobbles versus cores without cobbles by vehicle access type for Aldinga Bay beach sections (i.e. within-beach comparisons) and results of contingency tables tests for each sampling occasion (*n* = 9), year (*n* = 3) or season (*n* = 3). Bold text indicates significant associations between beach section types and cobble presence or absence. There was no data (n/d) for the pre-summer sampling occasion in year 3 because sediment cores were not collected on that occasion.

a)	3x2 tables	Year 1 Absent	Year 1 Present	Year 2 Absent	Year 2 Present	Year 3 Absent	Year 3 Present	Overall Absent	Overall Present
Mid-winter	Seasonal	**8**	**4**	**14**	**4**	5	13	27	21
	Bollarded	**3**	**3**	**13**	**5**	5	13	21	21
	Open	**3**	**15**	**4**	**14**	11	7	18	36
Pre-summer	Seasonal	7	11	**17**	**1**	n/d		**24**	**12**
	Bollarded	4	14	**8**	**10**			**12**	**24**
	Open	4	14	**10**	**8**			**14**	**22**
Post-summer	Seasonal	**18**	**0**	14	3	14	4	**46**	**7**
	Bollarded	**15**	**3**	14	4	14	4	**41**	**13**
	Open	**12**	**6**	9	9	10	8	**31**	**23**
Overall	Seasonal	**33**	**15**	**45**	**8**	19	17	**97**	**40**
	Bollarded	**22**	**20**	**35**	**19**	17	19	**74**	**58**
	Open	**19**	**35**	**23**	**31**	21	15	**63**	**81**

b)	Test statistics	Year 1 χ^2	Year 1 *P*	Year 2 χ^2	Year 2 *P*	Year 3 χ^2	Year 3 *P*	Overall χ^2	Overall *P*
Mid-winter	χ^2 for 2d.f.	**7.948†**	**0.019**	**13.784**	**0.001**	5.610	0.061	5.790	0.055
Pre-summer	χ^2 for 2d.f.	1.662	0.436	**10.881**	**0.004**	n/d		**9.236**	**0.010**
Post-summer	χ^2 for 2d.f.	**7.200†**	**0.027**	5.163	0.076	2.842	0.241	**12.087**	**0.002**
Overall	χ^2 for 2d.f.	**11.484**	**0.003**	**20.804**	**<0.001**	0.892	0.640	**20.952**	**<0.001**

† More than $^{1}/_{5}$ of cells were sparse – computed significance values are suspect

Appendix 3.4: Frequency of cores with cobbles versus cores without cobbles by vehicle access type for Moana Bay beach sections (i.e. within-beach comparisons), and results of contingency tables tests for each sampling occasion (*n* = 6). Bold text indicates significant associations between beach section types and cobble presence or absence. There was no data (n/d) for the pre-summer sampling occasion in year 3 because sediment cores were not collected on that occasion.

a) 3x2 tables		Year 2		Year 3		Overall	
		Absent	Present	Absent	Present	Absent	Present
Mid-winter	Closure	18	0	11	7	29	7
	Open	18	0	13	5	31	5
	Bollarded	18	0	15	3	33	3
Pre-summer	Closure	15	3	n/d		15	3
	Open	16	2			16	2
	Bollarded	18	0			18	0
Post-summer	Closure	18	0	18	0	36	0
	Open	18	0	17	1	35	1
	Bollarded	18	0	16	2	34	2
Overall	Closure	51	3	29	7	80	10
	Open	52	2	30	6	82	8
	Bollarded	54	0	31	5	85	5

b) Test statistics		χ^2	*P*	χ^2	*P*	χ^2	*P*
Mid-winter	$\chi^2_{\text{for 2d.f.}}$	0.000	1.000	2.215	0.330	1.858	0.394
Pre-summer	$\chi^2_{\text{for 2d.f.}}$	3.056†	0.214	n/d		3.086†	0.214
Post-summer	$\chi^2_{\text{for 2d.f.}}$	0.000	1.000	2.117	0.347	2.057†	0.358
Overall	$\chi^2_{\text{for 2d.f.}}$	2.889†	0.236	0.400	0.819	1.806	0.405

† More than $^1/_5$ of cells were sparse – computed significance values are suspect

Appendix 4.1: Measuring the realised sediment displacement by vehicles on a beach subject to intense vehicle usage over a period of several months: notes on field methods on a failed experiment with some findings

1. Background

Estimating displacement of sediment by vehicles on beaches using the controlled application of vehicle traffic is an invaluable exercise for quantifying potential loss via erosion due to vehicle actions on the beach-face (Anders & Leatherman 1987; Chapter 4). By this method, it has been shown that vehicles mobilise substantial volumes of sand via sediment rutting, and thus, via down-slope displacement, may represent significant potential for erosion (Anders & Leatherman 1987; Chapter 4). Unfortunately, it is not ethically responsible to simulate, under controlled experimental conditions, the natural state of vehicle usage on a particular beach; for example, for obvious reasons it is not possible to quantify the impacts of reckless driving on the beach-face in a scientific study. However, it may be of interest to have an understanding of the realised effects of sediment displacement and thus disruption of beach sediments by vehicles under normal vehicle usage conditions for both scientific understanding and management purposes.

The aim of this project was to develop a method to measure *in situ* the realised displacement of sediment on a metropolitan sandy beach subject to intense vehicle usage over the austral summer months (December – February). Methods used here were based on a similar study undertaken in a terrestrial habitat, investigating rates of sediment movement in desert piedmont surfaces (Persisco *et al.* 2005). By using numbered and painted pebbles, these authors were successfully able to quantify short-term sediment movement rates on piedmont surfaces and compare rates of movement among sites (Persisco *et al.* 2005). Thus, in this pilot study of vehicle impacts on beaches, individually-numbered metal markers were buried at a known depth and location in the beach face, were used with the aim of tracking the accretion, erosion or alongshore movement of the surface sediments on two sections of beach, one exposed to intense vehicle traffic during the study period and the second closed to vehicles year-round.

2. Methods

Study site

Moana Beach was selected to trial the methods for this experiment. As stated in Chapter 1 of this thesis, Moana Beach is divided into three sections based on vehicle usage, Moana North (closed to vehicles), Moana (open section) and Moana Bollards (also closed to vehicles; Figure 1.3). Moana and Moana Bollards sections were chosen for comparison. Both of these sections have similar summertime beach slopes, widths and sediment characteristics (averaged over three years; see Chapter 3). Both beach sections have backing dune systems. Moana receives high summertime vehicle usage (summertime track density = 1.1 ±0.2 tracks.m^{-1}; n = 7 transects), while vehicle usage of the bollard is minimal (summertime track density = 0.01 ±0.01 tracks.m^{-1}; n = 7 transects), generally restricted to council vehicles and the occasional non-compliant driver (see Chapter 2).

Field methods

Fieldwork for the trial experiment was undertaken during the austral summer of 2006/07, with the final experiment planned for the austral summer of 2007/08. Transects were established between 20-22nd Dec. 2006, and the pilot trial concluded on 14-16th May 2007. A summertime trial was selected because this is the peak time for vehicle usage on Moana Beach (see Chapter 2) and also a time of calm weather conditions with minimal beach erosion. Three across-shore transects were established haphazardly in each section and the location of each transect was marked discretely with an inconspicuous wooden post placed 1m above the top of each transect, in the fore-dune area. Transects were established using a tape measure and extended from the top of the intertidal beach (defined as the toe of the fore-dune, where terrestrial vegetation begins) to the swash limit at low tide (Figure A4.1.1). Orientation of the transect was measured with a compass. Basic surveyors equipment (Horizon 2024 dumpy level and staff) was then used to measure the beach profile in 2m increments from the dune toe to the swash limit.

On each transect a cross, comprising 20m along-shore and 20m across-shore transects (i.e. see Figure A4.1.1) was established, centred in either the high-, mid- or low-shore zone (as observed on the day and time of set-up, but generally crosses represented the upper, middle and lower sections of the

Figure A4.1.1: Diagram showing two hypothetical transects (thin solid lines) and two 20x20m crosses (thick solid lines) layout in the high- and mid-shore beach zones

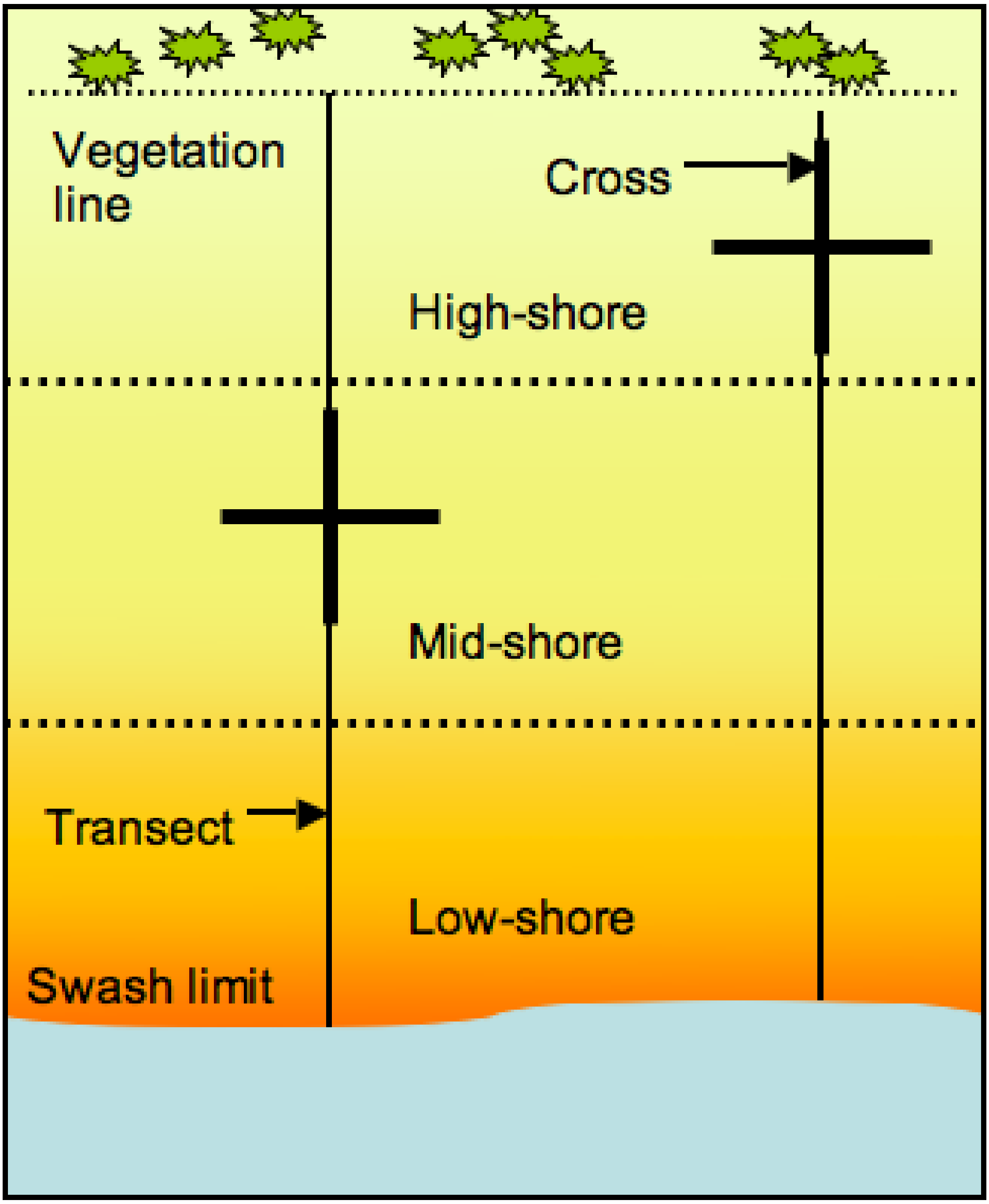

intertidal beach). Because it was uncertain if the pilot experiment would be successful and the time and cost associated with establishing each cross was great, only one cross was established per zone per site for the trial (purely to determine if the markers could be recovered after a 5-month deployment from various heights on the beach-face). A cross shape was selected because it provided a grid by which to track marker movements (i.e. with the centre of the cross [Figure A4.1.1] being the origin of a graphical plot of the area), thus allowing estimation of both along- and across-shore displacements (via markers placed at one level [along-shore arm] and across the beach [across-shore arm], respectively). The largest available (3.5cm diameter) zinc-plated washers, individually engraved with a tracking number, were used as markers for monitoring sediment movement. These markers could be detected when buried up to 30cm deep using a metal detector (Unbranded electronic treasure hunter SW-238; maximum detection depth for object the same size as markers = 35-40cm). The washers were selected as potentially suitable markers because, although they did not match the size or shape of the *in situ* sediments (i.e. small cobbles; sand grains would be impossible to simulate and detect), they were large enough to mark and could be detected when buried using a metal detector (see results). Markers could not be left on the sediment surface (*sensu* Persisco *et al.* 2005) because they most likely would have been collected by beach goers or dislodged by waves and hence lost. Markers were placed 20cm apart along each arm of the 20x20m cross, buried at a depth of 25cm below the sediment surface. This depth was selected based on practicality (i.e. within the detectable depth range of the metal detector). In total 1200 markers were buried across the six crosses. A 5cm diameter corer was used to dig the holes to place the markers, so that the sand could be replaced over the marker with minimal disturbance to the sediment layering. The surface profile of the 20x20m cross was measured to 1cm accuracy in 1m increments using surveyors equipment. The profiles were checked monthly throughout the period of the trial, occasionally with the metal detector to determine if the markers could be detected. Vehicle usage of the beach was monitored as per Chapter 2. Upon termination of the trial, the metal detector was used to search for markers, and the final location of any recovered markers was to be recorded by measuring the x- and y-axis components of distance from the origin of the cross and their depth of burial.

Calculations

Because each marker was individually numbered it was possible to precisely track the movement of the marker by considering the initial versus final burial locations as co-ordinates in 3D space and calculating the length and direction of the vector that connects them.

3. Results & Discussion

On termination of the experiment, no markers were detected from either section of the beach, even though they had been detected on visits during the trial with the metal detector. One marker had been observed on the surface during monthly visits to the site (from the high-shore of Moana Bollards transect 1 on 7/2/07). A second, more powerful metal detector (Minelab Explorer SE; frequency range 1.5kHz to 100kHz) was hired to see if the markers could be located but this was still unsuccessful. To test that the metal detectors could adequately find the markers buried in the sand, some left-over markers were buried by one field assistant at 25cm depth 20cm apart along a line and a 5x5m area searched with the metal detector (one trial for each detector) by a second assistant (who had no knowledge of the location of the line within the area). Both detectors successfully found the buried markers. Finally, it was attempted to find the markers by excavation (except Moana high-shore where the sand had been lost and only a cobble bed remained). An area extending 1m in all directions from the centre of where the cross had originally been located (i.e. $4m^2$) was excavated and the sand sieved through a 2mm mesh sieve, but still no markers were recovered. Because no markers were recovered at the termination of the trial, it was not possible to determine total movement of markers or displacement by this method on these beach sections.

Beach-face profile plots from the across-shore transects showed that all transects across both beach sections lost sediment over the five-month trial from the initial to the final profile measurement (Figure A4.1.2). This result was unexpected for a trial conducted over the summertime calm-weather period, during which beaches are expected to accrete sediment, not be eroded, especially as there were no major storm events during the marker deployment period (see Appendix 1). On average there was a 12.4±0.02 cm loss of beach height per linear metre of beach (i.e. less than the 25cm burial depth for markers), with the two sections showing equal losses (12.5±0.1 versus 12.4±0.05 cm/m for Moana & Moana Bollards, respectively). Beach profile plots

Figure A4.1.2: Beach profile plots showing initial beach-face profiles (Dec. 2006), initial marker burial depths and final beach-face profiles (May 2007) for each transect (*n* = 3) in both beach sections.

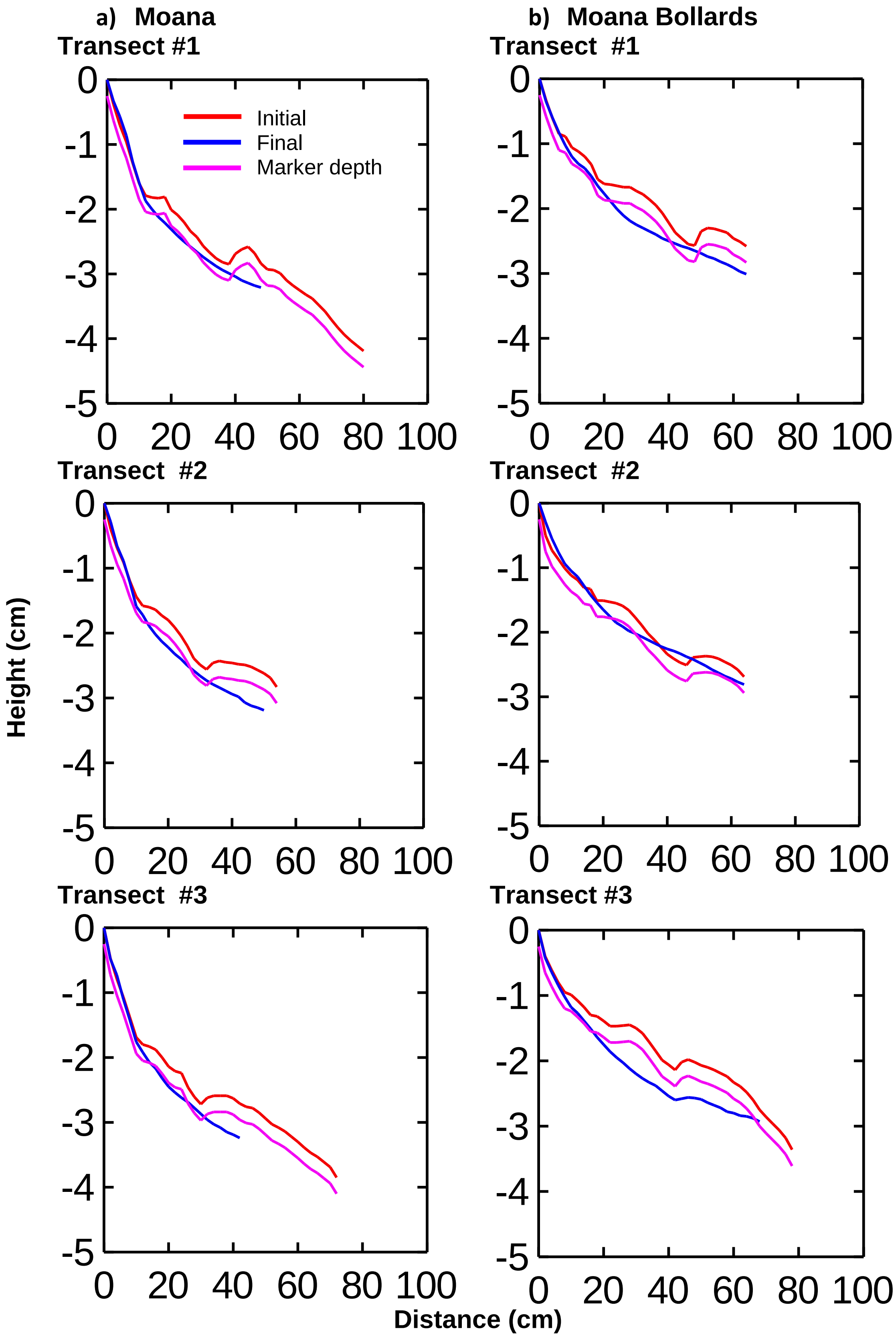

revealed that, for most of the transects (the exception being Moana Bollards transect #2), the final beach-face profile was often below the level of the marker burial depth except for the top 5-10m of the transect (high-shore zone), indicating a strong likelihood that most markers were probably lost via erosion of the beach-face due to wave action mobilising and reworking surface sediments, especially those buried in the mid- or low-shore zones. Significant reworking of the intertidal beach face is certainly indicated by the profile plots in Figure A4.1.2. However, even with erosion, some markers should have remained, for example those in the high-shore zone. None were found. There are many possible explanations for this disappointing observation, including:

1) over the five month trial, there may have been multiple, short-term erosion and accretion events in these beach sections, resulting the loss of sediment (and the markers) followed by deposition of sediment raising the height of the beach to near original levels (but not supported by storm events data; Appendix 1);
2) the high-shore zone of Moana Bay Beach consists of a sand-covered cobble bed, and by May much of the sand had been washed away (possibly including the buried markers) revealing the cobbles underneath, with little change in beach profile (i.e. cobbles provide an underlying and stable beach-face profile structure). Thus, any remaining markers may have fallen through the cobble bed;
3) some markers remained in the beach-face but were not found by the metal detector or trench digging upon termination of the trial, possibly these were moved laterally over long distances or vertically down by wave action; and
4) markers were found, collected or otherwise disrupted by beach-goers, some of whom use high-powered metal detectors to search for lost money and other valuable items on these popular beaches.

Both explanations 1, 2 and 3 rely on sediment movement on the beach being very great, regardless of vehicle access, thus this experiment may have been defeated by dynamism of the beach. This would also imply that vehicle effects may be trivial in relation to natural dynamism of the beach.

However the markers were lost, it still remains that this method was not successful at tracking sediment movements and measuring the actual displacement of sediment on beaches.

Appendix 5.1: Frequency of cores containing fauna by core cover and vehicle access type and results of contingency tables tests for each sampling occasion (*n* = 9), year (*n* = 3) or season (*n* = 3). Bold text indicates significant associations of fauna presence with both vehicle access (i.e. open versus closed beaches) and cover (i.e. bare sand versus wrack) types.

a) 2x2 tables		Year 1		Year 2		Year 3		Overall	
		Bare	Wrack	Bare	Wrack	Bare	Wrack	Bare	Wrack
Mid-winter	Closed	0	12	4	12	3	13	**7**	**37**
	Open	4	9	8	4	2	5	**18**	**18**
Pre-summer	Closed	9	17	9	17	2	4	20	38
	Open	1	5	3	2	3	3	7	10
Post-summer	Closed	2	17	5	11	5	9	12	37
	Open	0	4	0	1	0	1	0	6
Overall	Closed	11	46	**18**	**40**	10	26	39	112
	Open	5	18	**11**	**7**	5	9	21	34

b) Fishers Exact test statistics	Year 1	Year 2	Year 3	Overall
Mid-winter	0.096	0.053	0.621	**0.002**
Pre-summer	0.637	0.350	1.000	0.775
Post-summer	1.000	1.000	1.000	0.320
Overall	0.768	0.028	0.733	0.118

Appendix 5.2: Frequency of cores with fauna absent (i.e. a 'null' core) versus fauna present by vehicle access type and results of contingency tables tests for each sampling occasion (*n* = 9), year (*n* = 3) or season (*n* = 3). Bold text indicates significant associations of fauna presence or absence with vehicle access types (i.e. open versus closed beaches).

a) 2x2 tables

		Year 1		Year 2		Year 3		Overall	
		Absent	Present	Absent	Present	Absent	Present	Absent	Present
Mid-winter	Closed	24	12	20	16	**20**	**16**	64	44
	Open	23	13	24	12	**29**	**7**	76	32
Pre-summer	Closed	**10**	**26**	**10**	**26**	**31**	**5**	**50**	**58**
	Open	**30**	**6**	**31**	**5**	**18**	**18**	**91**	**17**
Post-summer	Closed	**17**	**19**	**20**	**16**	**22**	**14**	**59**	**49**
	Open	**32**	**4**	**35**	**1**	**35**	**1**	**102**	**6**
Overall	Closed	**51**	**57**	**50**	**58**	**72**	**36**	**173**	**151**
	Open	**85**	**23**	**90**	**18**	**94**	**14**	**269**	**55**

b) Fishers Exact test statistics

	Year 1	Year 2	Year 3	Overall
Mid-winter	1.000	0.469	**0.042**	0.117
Pre-summer	**<0.001**	**<0.001**	**0.002**	**<0.001**
Post-summer	**<0.001**	**<0.001**	**<0.001**	**0.000**
Overall	**<0.001**	**<0.001**	**<0.001**	**0.000**

Appendix 5.3: Frequency of cores containing fauna by vehicle access type for Aldinga Bay beach sections and results of contingency tables tests for each sampling occasion (*n* = 9), year (*n* = 3) or season (*n* = 3). Bold text indicates significant associations of fauna presence or absence with vehicle access sections.

a) 3x2 tables		Year 1		Year 2		Year 3		Overall	
		Absent	Present	Absent	Present	Absent	Present	Absent	Present
Mid-winter	Seasonal	**9**	**3**	**14**	**4**	18	0	**41**	**7**
	Bollarded	**6**	**0**	**15**	**3**	18	0	**39**	**3**
	Open	**8**	**10**	**6**	**12**	18	0	**32**	**22**
Pre-summer	Seasonal	17	1	13	5	**18**	**0**	48	6
	Bollarded	16	2	17	1	**17**	**1**	50	4
	Open	16	2	17	1	**13**	**5**	46	8
Post-summer	Seasonal	17	1	14	4	15	3	46	8
	Bollarded	15	3	17	1	16	2	48	6
	Open	18	0	17	1	17	1	52	2
Overall	Seasonal	43	5	41	13	51	3	**135**	**21**
	Bollarded	37	5	49	5	51	3	**137**	**13**
	Open	42	12	40	14	48	6	**130**	**32**
b) Test statistics		χ^2	*P*	χ^2	*P*	χ^2	*P*	χ^2	*P*
Mid-winter	$\chi^2_{\text{for 2d.f.}}$	**6.983**	**0.030**†	**11.856**	**0.003**	0.000	1.000†	**17.860**	**<0.001**
Pre-summer	$\chi^2_{\text{for 2d.f.}}$	0.441	0.802†	5.252	0.072†	**7.875**	**0.019**†	1.500	0.472
Post-summer	$\chi^2_{\text{for 2d.f.}}$	3.780	0.151†	3.375	0.185†	1.125	0.570	3.884	0.143
Overall	$\chi^2_{\text{for 2d.f.}}$	3.257	0.196	5.686	0.058	1.620	0.445	**7.982**	**0.018**

† More than $^1/_5$ of cells were sparse – computed significance values are suspect

Appendix 5.4: Frequency of cores containing fauna by vehicle access type for Moana Bay beach sections for years 2 and 3 only, and results of contingency tables tests for each sampling occasion (*n* = 6). Bold text indicates significant associations of fauna presence or absence with vehicle access sections.

c) 3x2 tables		Year 2		Year 3		Overall	
		Absent	Present	Absent	Present	Absent	Present
Mid-winter	Closure	**14**	**4**	15	3	29	7
	Open	**18**	**0**	11	7	29	7
	Bollarded	**10**	**8**	14	4	24	12
Pre-summer	Closure	**3**	**15**	**10**	**8**	**13**	**23**
	Open	**14**	**4**	**17**	**1**	**31**	**5**
	Bollarded	**5**	**13**	**16**	**2**	**21**	**15**
Post-summer	Closure	**15**	**3**	18	0	**33**	**3**
	Open	**18**	**0**	18	0	**36**	**0**
	Bollarded	**12**	**6**	16	2	**28**	**8**
Overall	Closure	**32**	**22**	43	11	**75**	**33**
	Open	**50**	**4**	46	8	**96**	**12**
	Bollarded	**27**	**27**	46	8	**73**	**35**
Test statistics		χ^2	*P*	χ^2	*P*	χ^2	*P*
Mid-winter	$\chi^2_{\text{for 2d.f.}}$	**10.286**	**0.006** †	2.507	0.285 †	2.533	0.282
Pre-summer	$\chi^2_{\text{for 2d.f.}}$	**15.801**	**<0.001**	**9.818**	**0.007** †	**18.857**	**<0.001**
Post-summer	$\chi^2_{\text{for 2d.f.}}$	**7.200**	**0.027** †	4.154	0.125 †	**9.919**	**0.007** †
Overall	$\chi^2_{\text{for 2d.f.}}$	**24.621**	**<0.001**	0.800	0.670	**16.167**	**<0.001**

† More than $^1/_5$ of cells were sparse – computed significance values are suspect

Appendix 5.5: Average similarities and abundances (4th root transformed) of up to the top 3 species (in order of higher to lower contribution) selected by SIMPER analysis as contributing (%C) the most to average similarity among samples (for all cover types) for beaches open or closed to vehicles, for each seasonal sampling occasion (MW: mid-winter; PS: pre-summer; PT: post-summer) and overall year (ALL) of the study. Low ratios of percent contribution to standard deviation (%C/SD) indicated that the consistency of occurrence of typifying species in samples were generally low, where this was not the case, entries have been **bolded**. Occasions with zero similarity (ZS) or no fauna (NF) are noted. Dashed spaces in place of species names indicate that no species were suggested of that rank.

Year	Season	Ave. Sim	Species 1	Abun	%C/C	%C	Species 2	Abun	%C/C	%C	Species 3	Abun	%C/C	%C
Moana (Open)														
1	MW	0.00	ZS											
	PS	0.00	ZS											
	PT	9.58	*Cafius australis*	0.20	0.35	100.00	-				-			
	ALL	2.48	*Cafius australis*	0.09	0.15	71.36	*T. quadrimana*	0.07	0.08	28.64	-			
2	MW	-	NF											
	PS	0.00	ZS											
	PT	-	NF											
	ALL	1.61	Scimyzidae larvae #1	0.04	0.13	100.00	-				-			
3	MW	13.84	Haustorius sp.	0.48	0.51	94.76	-				-			
	PS	0.00	ZS											
	PT	-	NF											
	ALL	7.59	Haustorius sp.	0.16	0.37	96.26	-				-			
Sellicks (Open)														
1	MW	30.76	*T. quadrimana*	0.89	0.73	100.00	-				-			
	PS	0.00	ZS											
	PT	-	NF											
	ALL	27.19	*T. quadrimana*	0.33	0.67	100.00	-				-			
2	MW	28.84	Haustorius sp.	0.77	0.68	67.68	Cumacean sp.	0.22	0.30	18.98	Chiltonia sp. 1	0.28	0.32	13.34
	PS	-	NF											
	PT	0.00	ZS											
	ALL	22.06	Haustorius sp.	0.26	0.62	78.58	Chiltonia sp. 1	0.09	0.26	11.49	-			
3	MW	-	NF											
	PS	9.85	Haustorius sp.	0.30	0.30	71.80	*T. quadrimana*	0.11	0.17	28.20	-			
	PT	0.00	ZS											
	ALL	3.85	Haustorius sp.	0.10	0.18	71.80	*T. quadrimana*	0.04	0.10	28.20	-			

Appendix 5.5: cont.

Year	Season	Ave. Sim.	Species 1	Abun	%C/C	%C	Species 2	Abun	%C/C	%C	Species 3	Abun	%C/C	%C
Maslin (Closed)														
1	MW	41.27	***T. quadrimana***	**0.54**	**1.12**	**92.30**	-				-			
	PS	12.93	Mecoptera larvae #1	0.36	0.37	28.57	*Actaecia pallida*	0.52	0.35	26.81	*T. quadrimana*	0.55	0.37	25.85
	PT	55.14	***Cafius australis***	**0.60**	**1.67**	**57.44**	***Actaecia pallida***	**0.58**	**1.11**	**42.56**	-			
	ALL	14.51	*T. quadrimana*	0.36	0.32	34.54	*Actaecia pallida*	0.36	0.34	27.07	*Cafius australis*	0.30	0.30	24.32
2	MW	8.63	*T. quadrimana*	0.28	0.40	100.00	-				-			
	PS	11.66	*Actaecia pallida*	0.36	0.32	49.21	Tricopteran larvae #2	0.30	0.32	37.54	*Hyocis bakewelli (?)*	0.11	0.13	10.03
	PT	12.63	*Actaecia pallida*	0.30	0.36	85.12	*T. quadrimana*	0.11	0.14	7.61	-			
	ALL	8.38	*Actaecia pallida*	0.22	0.29	65.15	**Tricopteran larvae #2**	**0.10**	**1.52**	**0.18**	*T. quadrimana*	0.16	0.12	9.58
3	MW	27.93	*T. quadrimana*	0.68	0.73	100.00	-				-			
	PS	0.00	ZS											
	PT	12.62	*T. quadrimana*	0.25	0.41	69.74	*Cafius australis*	0.20	0.29	23.97	-			
	ALL	9.63	*T. quadrimana*	0.35	0.36	88.46	*Actaecia pallida*	0.08	0.12	6.06	-			
Port Willunga (Closed)														
1	MW	15.43	*T. quadrimana*	0.23	0.49	100.00	-				-			
	PS	30.43	*T. quadrimana*	0.65	0.73	78.33	*Aphela phalerioides*	0.38	0.45	21.67	-			
	PT	21.74	*Cafius australis*	0.45	0.62	52.90	*Actaecia pallida*	0.24	0.36	20.88	*T. quadrimana*	0.28	0.36	15.58
	ALL	15.53	*T. quadrimana*	0.39	0.41	61.68	*Cafius australis*	0.17	0.26	18.33	*Aphela phalerioides*	0.17	0.22	12.94
2	MW	51.24	***T. quadrimana***	**1.26**	**1.33**	**95.05**	-				-			
	PS	27.75	*T. quadrimana*	0.84	0.78	86.33	*Aphela phalerioides*	0.30	0.23	6.70	-			
	PT	9.84	*Cafius australis*	0.26	0.38	60.48	*Aphela phalerioides*	0.22	0.26	29.73	-			
	ALL	24.57	*T. quadrimana*	0.72	0.69	87.77	*Aphela phalerioides*	0.23	0.19	5.75	-			
3	MW	25.34	*T. quadrimana*	0.55	0.71	79.94	*Cirolana corpulenta*	0.29	0.36	12.19	-			
	PS	8.58	*T. quadrimana*	0.22	0.33	100.00	-				-			
	PT	8.58	*Aphela phalerioides*	0.43	0.35	72.35	*Actaecia pallida*	0.27	0.24	22.19	-			
	ALL	10.14	*T. quadrimana*	0.30	0.28	44.52	*Aphela phalerioides*	0.26	0.26	35.82	*Cirolana corpulenta*	0.10	0.18	10.99

Appendix 5.6: Average similarities and average abundances (4th root transformed) of up to the tree species selected by SIMPER analysis as contributing (%C) the most to average similarity (in order of higher to lower contribution) among samples (for all cover types) for Aldinga Bay beach sections, for each seasonal sampling occasion (as for Appendix 5.5) and overall year. Low ratios of percent contribution to standard deviation (%C/SD) indicated that the consistency of occurrence of typifying species in samples were generally low, where this was not the case, entries have been **bolded**. Occasions with zero similarity (ZS) or no fauna (NF) are noted. Dashed spaces in place of species names indicate that no species were suggested of that rank.

Year	Season	Ave. Sim.	Species 1	Abun	%C/C	%C	Species 2	Abun	%C/C	%C	Species 3	Abun	%C/C	%C
Seasonal closure														
1	MW	23.56	*T. quadrimana*	0.27	0.55	100.00	-				-			
	PS	0.00	ZS											
	PT	0.00	ZS											
	ALL	4.42	*T. quadrimana*	0.07	0.22	100.00	-				-			
2	MW	0.00	ZS											
	PS	0.00	ZS											
	PT	11.54	***Paphies elongata***	**0.17**	**1.31**	**100.00**	-				-			
	ALL	2.34	*Paphies elongata*	0.06	0.15	100.00	-				-			
3	MW	-	NF											
	PS	-	NF											
	PT	14.29	*Aphela phalerioides*	0.17	0.40	100.00	-				-			
	ALL	6.25	*Aphela phalerioides*	0.06	0.26	100.00	-				-			
Bollarded closure														
1	MW	-	NF											
	PS	2.67	*Aphela phalerioides*	0.11	0.26	100.00	-				-			
	PT	0.00	ZS											
	ALL	0.80	*Aphela phalerioides*	0.05	0.14	100.00	-				-			
2	MW	-	NF											
	PS	0.00	ZS											
	PT	0.00	ZS											
	ALL	0.00	ZS											
3	MW	-	NF											
	PS	0.00	ZS											
	PT	0.00	ZS											
	ALL	0.00	ZS											

Appendix 5.6: cont.

Year	Season	Ave. Sim.	Species 1	Abun	%C/C	%C	Species 2	Abun	%C/C	%C	Species 3	Abun	%C/C	%C
Open														
1	MW	30.76	*T. quadrimana*	0.89	0.73	100.00	-				-			
	PS	0.00	ZS											
	PT	-	NF											
	ALL	27.19	*T. quadrimana*	0.33	0.67	100.00	-				-			
2	MW	28.84	*Haustorius sp.*	0.77	0.68	67.68	Cumacean sp.	0.22	0.30	18.98	*Chiltonia sp. 1*	0.28	0.32	13.34
	PS	-	NF											
	PT	0.00	ZS											
	ALL	22.06	*Haustorius sp.*	0.26	0.62	78.58	*Chiltonia sp. 1*	0.09	0.26	11.49	-			
3	MW	-	NF											
	PS	9.85	*Haustorius sp.*	0.30	0.30	71.80	*T. quadrimana*	0.11	0.17	28.20	-			
	PT	0.00	ZS											
	ALL	3.85	*Haustorius sp.*	0.10	0.18	71.80	*T. quadrimana*	0.04	0.10	28.20	-			

Appendix 5.7: Average similarities and average abundances (4th root transformed) of the tree species selected by SIMPER analysis as contributing (%C) the most to average similarity (in order of higher to lower contribution) among samples (for all cover types) for Moana Bay beach sections, for each seasonal sampling occasion (as for Appendix 5.5) and overall year. Low ratios of percent contribution to standard deviation (%C/SD) indicated that the consistency of occurrence of typifying species in samples were low. Occasions with zero similarity (ZS) or no fauna (NF) are noted. Dashed spaces in place of species names indicate that no species were suggested of that rank.

Year	Season	Ave. Sim.	Species 1	Abun	%C/C	%C	Species 2	Abun	%C/C	%C	Species 3	Abun	%C/C	%C
Closed														
2	MW	1.93	*T. quadrimana*	0.18	0.21	100.00	-				-			
	PS	25.55	*T. quadrimana*	0.70	0.62	57.89	*Aphela phalerioides*	0.47	0.51	31.09	*Sciomyzidae larvae #1*	0.44	0.24	6.02
	PT	4.29	*T. quadrimana*	0.11	0.22	55.56	*Aphela phalerioides*	0.11	0.22	44.44	-			
	ALL	16.43	*T. quadrimana*	0.33	0.47	62.31	*Aphela phalerioides*	0.19	0.34	24.97	*Sciomyzidae larvae #1*	0.15	0.20	6.73
3	MW	0.00	ZS											
	PS	8.78	*T. quadrimana*	0.43	0.38	100.00	-				-			
	PT		NF											
	ALL	3.96	*T. quadrimana*	0.14	0.26	100.00	-				-			
Open														
2	MW		NF											
	PS	0.00	ZS											
	PT		NF											
	ALL	1.61	Scimyzidae larvae #1	0.04	0.13	100.00	-				-			
3	MW	13.84	*Haustorius sp.*	0.48	0.51	94.76	-				-			
	PS	0.00	ZS											
	PT		NF											
	ALL	7.59	*Haustorius sp.*	0.16	0.37	96.26	-				-			
Bollarded														
2	MW	19.43	*Haustorius sp.*	0.41	0.53	100.00	-				-			
	PS	25.85	*T. quadrimana*	0.64	0.64	55.97	*Cafius australis*	0.65	0.54	42.02	-			
	PT	6.21	*Actaecia pallida*	0.12	0.16	35.89	*Cafius australis*	0.19	0.28	29.90	*Trachyscelis ciliaris*	0.11	0.16	14.27
	ALL	15.98	*T. quadrimana*	0.23	0.37	37.14	*Haustorius sp.*	0.14	0.25	34.59	*Cafius australis*	0.28	0.30	24.31
3	MW	2.58	Chiltonia sp.	0.24	0.19	100.00	-				-			
	PS	5.76	*T. quadrimana*	0.13	0.26	100.00	-				-			
	PT	0.00	ZS											
	ALL	2.95	Chiltonia sp.	0.08	0.15	42.72	*Scymena amphibia*	0.04	0.09	26.45	*T. quadrimana*	0.04	0.09	22.84

Appendix 6.1: Taxonomy of nematode worms collected from study beaches, to Order, but only Genus names for some species (Platt & Warwick 1983; 1988; Warwick *et al.* 1998). Feeding guilds, based on buccal cavity structure (Jensen 1987) are also given.

Name	Order	Genus	Feeing Guild
Chromadora sp.	Enoplida	*Chromadora*	Deposit feeder
Steineria sp.	Enoplida	*Steineria*	Deposit feeder
Paradontophora sp. 1	Enoplida	*Paradontophora*	Scavenger
Paradontophora sp. 2	Enoplida	*Paradontophora*	Epistrate feeder
Retrotheristus	Enoplida	*Retrotheristus*	Epistrate feeder
Viscosia sp.	Enoplida	*Viscosia*	Predator
Enlopid sp.1	Enoplida	sp. 1	Deposit feeder
Enlopid sp.2	Enoplida	sp. 2	Epistrate feeder
Enlopid sp.3	Enoplida	sp. 3	Deposit feeder
Enlopid sp.4	Enoplida	sp. 4	Deposit feeder
Enlopid sp.5	Enoplida	sp. 5	Deposit feeder
Enlopid sp.6	Enoplida	sp. 6	Predator
Enlopid sp.7	Enoplida	sp. 7	Deposit feeder
Enlopid sp.8	Enoplida	sp. 8	Deposit feeder
Enlopid sp.9	Enoplida	sp. 9	Predator
Enlopid sp.10	Enoplida	sp. 10	Deposit feeder
Enlopid sp.11	Enoplida	sp. 11	Deposit feeder
Enlopid sp.12	Enoplida	sp. 12	Deposit feeder
Enlopid sp.13	Enoplida	sp. 13	Omnivore
Enlopid sp.14	Enoplida	sp. 14	Deposit feeder
Enlopid sp.15	Enoplida	sp. 15	Predator
Enlopid sp.16	Enoplida	sp. 16	Epistrate feeder
Enlopid sp.17	Enoplida	sp. 17	Deposit feeder
Enlopid sp.18	Enoplida	sp. 18	Deposit feeder
Enlopid sp.19	Enoplida	sp. 19	Deposit feeder
Enlopid sp.20	Enoplida	sp. 20	Predator
Enlopid sp.21	Enoplida	sp. 21	Deposit feeder
Enlopid sp.22	Enoplida	sp. 22	Deposit feeder
Enlopid sp.23	Enoplida	sp. 23	Predator
Nudora sp.	Monhysterida	*Nudora*	Deposit feeder
Monhysterid sp.1	Monhysterida	sp. 1	Deposit feeder
Monhysterid sp.2	Monhysterida	sp. 2	Epistrate feeder
Monhysterid sp.3	Monhysterida	sp. 3	Predator
Monhysterid sp.4	Chromadorida	sp. 4	Epistrate feeder
Monhysterid sp.5	Monhysterida	sp. 5	Deposit feeder
Epsilonema sp.	Chromadorida	*Epsilonema*	Deposit feeder
Chromadorid sp.1	Chromadorida	sp. 1	Deposit feeder
Chromadorid sp.2	Chromadorida	sp. 2	Omnivore
Chromadorid sp.3	Chromadorida	sp. 3	Predator
Chromadorid sp.4	Chromadorida	sp. 4	Predator

Appendix 6.2: Summary tables for results of ANOVA tests on measured sediment variables (all square-root transformed to meet the assumptions for ANOVA; MGS [μm]: mean grain size; percent moisture: moisture (%); BD [g/mL]: bulk density; PR [kg/cm^2]: penetration resistance and PC [mL/cm^2/s]: percolation rate) and meiofaunal abundance and species richness (SR; both square-root transformed to meet the assumptions for ANOVA) for a) nested 3-factor ANOVA between-beaches, and for 2-factor ANOVA within-beaches (n = 45 samples) at b) Aldinga; and c) Moana Bays. Significance values are indicated with asterisks (p values: * < 0.05; ** < 0.01; blank = NS).

a) Open v. closed beaches

Variable:	MGS	Sorting	Moisture	BD	PR	PC	Abundance	SR
T	*							
S								*
T*S								
B(T)	**	**	**		**	**	**	**
S*B(T)	**	**	**		**	**	**	*

b) Aldinga Bay beach sections

Variable:	MGS	Sorting	Moisture	BD	PR	PC	Abundance	SR
T	***				***	***		***
S	***	***	***		***	**	***	***
T*S	***		***	*	***	***	*	***

c) Moana Bay beach sections

Variable:	MGS	Sorting	Moisture	BD	PR	PC	Abundance	SR
T	**		**	***	*		***	***
S		***	**	***	**	***	*	**
T*S	***		***	***	***	**	***	***